Soluble, light-absorbing species in snow at Barrow, Alaska

Harry Beine,[1] Cort Anastasio,[1] Giulio Esposito,[2] Kelley Patten,[1] Elizabeth Wilkening,[3] Florent Domine,[4,5] Didier Voisin,[4] Manuel Barret,[4] Stephan Houdier,[4] and Sam Hall[6]

Received 29 April 2011; revised 23 June 2011; accepted 1 July 2011; published 28 September 2011.

[1] As part of the international multidisciplinary Ocean - Atmosphere - Sea Ice - Snowpack (OASIS) program we analyzed more than 500 terrestrial (melted) snow samples near Barrow, AK between February and April 2009 for light absorption, as well as H_2O_2 and inorganic anion concentrations. For light absorption in the photochemically active region (300–450 nm) of surface snows, H_2O_2 and NO_3^- make minor contributions (combined < 9% typically), while HUmic LIke Substances (HULIS) and unknown chromophores each account for approximately half of the total absorption. We have identified four main sources for our residual chromophores (i.e., species other than H_2O_2 or NO_3^-): (1) vegetation and organic debris impact mostly the lowest 20 cm of the snowpack, (2) marine inputs, which are identified by high Cl^- and SO_4^{2-} contents, (3) deposition of diamond dust to surface snow, and (4) gas-phase exchange between the atmosphere and surface snow layers. The snow surfaces, and accompanying chromophore concentrations, are strongly modulated by winds and snowfall at Barrow. However, even with these physical controls on light absorption, we see an overall decline of light absorption in near-surface snow during the 7 weeks of our campaign, likely due to photo-bleaching of chromophores. While HULIS and unknown chromophores dominate light absorption by soluble species in Barrow snow, we know little about the photochemistry of these species, and thus we as a community are probably overlooking many snowpack photochemical reactions.

Citation: Beine, H., C. Anastasio, G. Esposito, K. Patten, E. Wilkening, F. Domine, D. Voisin, M. Barret, S. Houdier, and S. Hall (2011), Soluble, light-absorbing species in snow at Barrow, Alaska, *J. Geophys. Res.*, *116*, D00R05, doi:10.1029/2011JD016181.

1. Introduction

[2] Snowpacks are photochemically active, both as sources of compounds such as NO_x, HONO, and oxidants or oxidant precursors (e.g., H_2O_2 and CH_2O), as well as sinks for species such as ozone [*Grannas et al.*, 2007, and references therein]. Compounds formed in the snowpack can be emitted into the overlying air, where they can alter the oxidative capacity of the boundary layer, or they can react within the snowpack, either on snow grains or in the interstitial firn air.

[3] Snow photochemical reactions in the snowpack are initiated by the absorption of actinic flux by chromophores (light-absorbing species) on/in snow grains in the photic zone of the snow. For example, photolysis of nitrate (NO_3^-) and nitrite (NO_2^-) in/on snow grains, quasi-liquid layers or the bulk ice leads to the release of NO_x ($NO + NO_2$) from snowpacks, while nitrate photolysis, perhaps especially in the presence of organic/humic material, can lead to the release of HONO [*Beine et al.*, 2006, 2008; *Grannas et al.*, 2007, and references therein; *Anastasio and Chu*, 2009; *Bartels-Rausch et al.*, 2010]. The mechanisms responsible for the release of organic compounds, such as aldehydes and ketones, from the snowpack are not yet fully understood, but likely involve thermal desorption of adsorbed species and out-diffusion of species that form a solid solution with ice, such as formaldehyde [*Barret et al.*, 2011a, 2011b] in addition to photochemical reactions [*Grannas et al.*, 2007, and references therein].

[4] The photochemical release of carbonyls likely involves breaking large, low volatility, organic/humic compounds in/on snow grains into smaller, volatile fragments. This could occur either via direct photodegradation of the organic chromophores or through indirect photoreactions of organics with oxidants such as hydroxyl radical (OH), which in snow is primarily formed from the photolysis of snow-grain hydrogen peroxide [*Anastasio et al.*, 2007; *Chu and Anastasio*, 2005; *Domine and Shepson*, 2002]. Large snow grain organics that may be found in terrestrial snowpacks include HUmic LIke

[1]Department of Land, Air, and Water Resources, University of California at Davis, Davis, California, USA.
[2]CNR – IIA, Rome, Italy.
[3]Wilson K8 School, Tucson, Arizona, USA.
[4]Laboratoire de Glaciologie et Géophysique de l'Environnement, CNRS-INSU and Université Joseph Fourier, Saint-Martin d'Hères, France.
[5]CNRS UMI 3376 Takuvik, Université Laval, Pavillon Alexandre Vachon, Quebec, Quebec, Canada.
[6]Atmosphere and Chemistry Division, NCAR, Boulder, Colorado, USA.

0148-0227/11/2011JD016181

Substances (HULIS) as well as electron rich phenolic and polyaromatic chromophores [*George et al.*, 2005; *Grannas et al.*, 2004]. The mixture of organic compounds in snow is complex and the identities of the major compounds and functional groups are largely uncharacterized [*Grannas et al.*, 2006].

[5] To fully understand photochemistry in snow we must identify the relevant photochemical reactions and quantify their rates. This includes determining the identities, concentrations and location of the major chromophores, as well as the photon flux at that location. The exact location of chemical compounds in the snowpack is still the topic of ongoing research; the co-location of chemicals in various snow reservoirs, such as quasi-liquid layers or the bulk ice, likely has important effects on solute reactivity [*Domine and Shepson*, 2002; *Domine et al.*, 2008 and references therein]. While actinic fluxes have been measured in high-latitude and high altitude snowpacks [*Beine et al.*, 2006; *France et al.*, 2011; *Galbavy et al.*, 2007a, 2007b; *King et al.*, 2005; *Lee-Taylor and Madronich*, 2002; *Simpson et al.*, 2002], much less is known about snow grain chromophores. The dominant light-absorbing species in snowpacks is the ice of snow grains, while insoluble impurities such as soot and soil dust make the second largest contribution [*Doherty et al.*, 2010; *Grenfell and Warren*; 2009; *Hagler et al.*, 2007; *Lee-Taylor and Madronich*, 2002; *Warren*, 1982; *Doherty et al.*, 2010]. Although ice absorption is important for the radiative balance of snowpacks, this absorption does not lead to chemical reaction and thus does not contribute to snow photochemistry. Soluble impurities, on the other hand, account only for a small portion of the sunlight that is absorbed by snowpacks, but probably play major roles in initiating snowpack photochemistry. However, with the exceptions of NO_3^- and H_2O_2, we know little about the identities of snow-grain chromophores, their contributions to light absorption, or their chemistries.

[6] As a first step in constraining the photochemistry of soluble snowpack chromophores, *Anastasio and Robles* [2007] quantified the light absorption by dissolved chromophores in 21 melted and filtered snow samples from Summit, Greenland, and Dome C, Antarctica. At both sites, NO_3^- and H_2O_2 together accounted for approximately half of the summed light absorption coefficients for wavelengths above 280 nm, while the remaining 50% of light absorption was due to unknown, probably organic, chromophores. At Summit, the amount of sunlight absorption by the unknown chromophores in the snow varied significantly over the course of the one day examined, with maximum values during morning and evening, and minimum values during midday and afternoon. This diurnal dependence of the unknown chromophores was similar to, but more dramatic than, previously described diurnal changes in snowpack H_2O_2 and formaldehyde due to exchange with the boundary layer [*Hutterli et al.*, 2001; *Jacobi et al.*, 2002]. The diurnal dependence of sunlight absorption by unknown chromophores suggests that approximately half of the unknown chromophore pool is either emitted from the snowpack into the boundary layer during the day (and then redeposited at night) or undergoes rapid photochemical losses during the early portion of the day. In either case these fluxes or reactions of the unknown, likely organic, light-absorbing species probably affect the composition and chemistry of both the surface snow as well as the lower atmosphere.

[7] As a second step in quantifying and characterizing light absorption by soluble chemical species in snow, we recently made extensive measurements of snow absorption as part of the international multidisciplinary Ocean - Atmosphere - Sea Ice - Snowpack (OASIS) campaign in Barrow, Alaska. This program studies chemical and physical exchange processes between the title reservoirs. It focuses on their impact on tropospheric chemistry and climate, as well as on the surface/biosphere and their feedbacks in the Arctic. Central to the interdisciplinary field study at Barrow, AK, to which 27 research groups from the U.S., Canada, France, UK, and Germany contributed, was the quantitative and reliable determination of chemical and biological fluxes to and from ice and snow surfaces, as a function of the nature of the surface and other relevant environmental conditions.

[8] As part of this campaign, we analyzed Barrow snow samples for light absorption by soluble chromophores, as well as for the concentrations of H_2O_2, nitrate, and other inorganic anions. To help us determine and quantify the prevalence and relative significance of chromophores, we made our light absorption measurements in concert with other measurements during the OASIS campaign, including snowpack physical parameters (F. Domine et al., Physical properties of the Arctic snowpack during OASIS, submitted to *Journal of Geophysical Research*, 2011; hereinafter Domine et al. submitted manuscript, 2011a) boundary layer meteorology (R. M. Staebler et al., Turnipseed, flux gradient relationships over the Arctic snowpack, submitted to *Journal of Geophysical Research*, 2011), aldehydes [*Barret et al.*, 2011b] and HULIS in the snow (D. Voisin et al., Carbonaceous species and Humic Like Substances (HULIS) in arctic snowpack during OASIS field campaign, submitted to *Journal of Geophysical Research*, 2011), snow optical measurements (J. L. France et al., Hydroxyl radical and nitrogen dioxide production rates, black carbon concentrations and light-absorbing impurities from field measurements of light penetration and nadir reflectivity of on-shore and off-shore coastal Alaskan snow, submitted to *Journal of Geophysical Research*, 2011), surface snow chemistry (F. Domine et al., The specific surface area and chemical composition of diamond dust near Barrow, Alaska, submitted to *Journal of Geophysical Research*, 2011; hereinafter Domine et al., submitted manuscript, 2011b) and HONO measurements in air and snow (G. Villena et al., Nitrous acid (HONO) in polar regions: A net source of OH radicals?, submitted to *Journal of Geophysical Research*, 2011).

[9] In the big picture, we are interested in the sources, nature, and potential fates of unknown chromophores that absorb tropospheric sunlight (especially between 300 and 450 nm) in order to begin to more fully understand photochemical reactions in snowpacks. For the OASIS campaign we were specifically interested in the following questions: What is the relative importance of known (H_2O_2, NO_3^-, and NO_2^-) and unknown soluble chromophores in Barrow surface snow? Are the unknown chromophores primarily organic species? What are the origins and lifetimes of snow chromophores? Are exchange processes important, either between the snow and the overlying atmosphere or in between different snow layers? And, finally, which processes help modulate chromophore concentrations in the

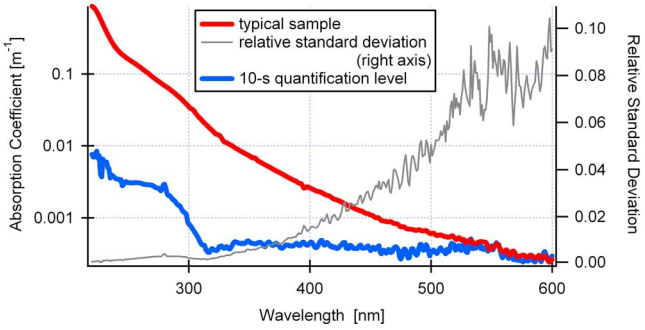

Figure 1. Typical absorption spectrum for terrestrial Barrow snow (prior to subtraction of offset). Over 90% of all samples show a spectrum with a similar shape to the red trace, with a typical absorption coefficient of 01–0.15 m^{-1} at 250 nm. The gray trace shows the relative standard deviation (right axis), and the blue curve shows the resulting system 10-σ quantification level.

snowpacks? In this paper we focus on light absorption in surface snowpacks on land, while a future companion paper will explore light absorption and chromophores in frost flowers and marine snow and ice samples (H. J. Beine et al., Soluble chromophores in marine snow, sea water, sea ice, and frost flowers near Barrow, Alaska, submitted to *Journal of Geophysical Research*, 2011).

2. Experiment

2.1. Sampling at Barrow, Alaska

[10] We collected over 500 snow samples during the OASIS field campaign at Barrow, Alaska, between February 27, and April 15, 2009 in the area around 156°39′35″W and 71°19′22″N, approximately 1000 m ESE of the Barrow Alaska Research Center (BARC). Undisturbed snow was sampled as described by *Domine and Shepson* [2002] and *Domine et al.* [2004], using polyethylene gloves and full-body Tyvek suits to avoid contamination. Samples were collected directly into pre-cleaned 100 mL Schott glass bottles. Our sampling plan included spatial and depth surveys (Domine et al., submitted manuscript, 2011a; Voisin et al., submitted manuscript, 2011) as well as daily snow profiles of the top 10 cm at sunrise, mid-day and sunset. Our daily sampling efforts were coordinated with other OASIS sampling whenever possible [*Barret et al.*, 2011a; Domine et al., submitted manuscript, 2011a, 2011b; Voisin et al., submitted manuscript, 2011; T. A. Douglas et al., Frost flowers growing in the Arctic ocean atmosphere sea ice interface: 1. Chemical composition and formation history, submitted to *Journal of Geophysical Research*, 2011]. Samples were stored at −20°C for up to a couple of days, if necessary.

2.2. LWCC UV-vis Analysis

[11] Samples were slowly melted (in the capped bottles) immediately prior to light absorption measurements. After melting was complete, we saved and refroze aliquots of each sample for later analysis for H_2O_2 and major anions (in our lab in Davis, CA), and measured UV-vis absorption in the field. Our spectrometer at Barrow consisted of a Deuterium Lamp (D2H, WPI), a 100-cm liquid wave core guide (LWCC) (WPI) and a TIDAS 1 (J&M) spectrometer. Before and after each sample spectrum a reference spectrum of purified water was recorded. Our purified water ("MQ") was obtained from the Barrow Arctic Science Consortium's (BASC) Milli-Q Plus system (≥ 18.2 MΩ cm). This reference was both recorded for quality control and used by the TIDASDaq software as a baseline for the subsequent sample. Thus no manual subtraction of a baseline is required and light absorption due to water is removed from our sample spectra by the instrument software. For additional reference and quality control we compared all MQ water spectra measured during the campaign to a single batch of higher purity "UV-MQ" water from our lab in Davis that was analyzed in Barrow. We prepared this UV-MQ water by adding H_2O_2 (final concentration of 500 μM) to fresh MQ in quartz tubes and illuminating with sixteen 45-W 254 nm UV lamps (Rayonet photochemical reactor, lamp #3020; The Southern New England Ultraviolet Company) for 24 h.

[12] We introduced melted snow samples and blanks into the LWCC after filtering through an inline 0.22 μm Teflon disposable syringe filter (Cameo), and we recorded spectra between 220 and 600 nm using the TIDASDaq software at 20 Hz for a duration of 60 to 120 s. Each spectrum was thus recorded with numerous (1200–2400) replicates; the spectra were saved as 3D files. Spectra and statistics were extracted using IGOR Macro routines. An example of the raw data treatment is shown in auxiliary material Figure S1.[1]

[13] The resulting spectrophotometer measurement at each wavelength λ is the base-10 light extinction (K_λ) (i.e., the sum of absorption and scattering), measured in our spectrophotometer as $K_\lambda = \log 1_0(I_0/I)$, where I_0 is the light intensity incident upon the solution and I is the light intensity transmitted through the solution. We convert each measured extinction value to a path length-normalized extinction coefficient (κ_λ) by dividing by the LWCC path length (l = 1 m):

$$\kappa_\lambda = K_\lambda / l \quad (1)$$

During the first week of the campaign several samples were taken in triplicate and analyzed separately. The resulting spectra were identical within our uncertainty (see below). For the remainder of the campaign each sample was thus routinely only taken once.

[14] Between 320 and 550 nm our 10-σ quantification level was on the order of 0.5×10^{-3} m^{-1} (Figure 1). Our measured absorption values were well above the 10-σ quantification level for wavelengths lower than approximately 500 nm, and similar to the 10-σ quantification level at longer wavelengths. We expect little or no sample light absorption at these long wavelengths [*Anastasio and Robles*, 2007], but this range is useful in determining whether the entire absorption spectrum is offset from zero, which happens frequently. In order to correct for this baseline offset, for each sample we determined the average extinction coefficient between 500 and 600 nm and subtracted this value from the value of κ_λ at every wavelength, as described below. The median offset was 1.1×10^{-3} m^{-1}, while 90% of

[1] Auxiliary material data sets are available at ftp://ftp.agu.org/apend/jd/2011jd016181. Other auxiliary material files are in the HTML. doi:10.1029/2010JD016181.

all offset values were below 5×10^{-3} m^{-1}. We also explored the possibility that the offset in our spectra above 500 nm was due to light extinction by particulate elemental carbon. Using molar absorptivities for elemental carbon (T. Kirchstetter, personal communication, 2009), 95% of the offset values correspond to elemental carbon concentrations below 10 ng/L, which is several orders of magnitude lower than measured black carbon concentrations in Arctic snows [*Doherty et al.*, 2010; *Grenfell and Warren*, 2009; France et al., submitted manuscript, 2011]. This suggests that our sample filtration was quite effective at removing black carbon and other particles from our samples.

[15] After correcting for their baseline offset, *Anastasio and Robles* [2007] assumed that extinction at wavelengths above approximately 400 nm was due to scattering and used an empirical fit to estimate the contribution of scattering at shorter wavelengths. We find here, however, that extinction at these long wavelengths is primarily due to light absorption by dissolved HUmic-Like Substances (HULIS), which were not measured by *Anastasio and Robles* [2007]: for our Barrow samples the median HULIS signal between 500–600 nm is 0.86×10^{-3} m^{-1} (Voisin et al., submitted manuscript, 2011). The HULIS contribution throughout the photochemically relevant wavelength region is explored in detail below. Thus we find no evidence of significant scattering in our samples (consistent with the fact that we filtered our samples) and we have not processed our data to remove an assumed scattering component. Our Barrow results suggest that the scattering "correction" of *Anastasio and Robles* [2007] therefore somewhat underestimated light absorption in their samples.

[16] We subtracted the baseline offset in each sample to arrive at the base-10 light absorption coefficient (α_λ) (see also auxiliary material Figure S1):

$$\alpha_\lambda = \kappa_\lambda - \text{Baseline Offset}_{(500-600nm)} \quad (2)$$

Note that the absorption coefficient α_λ represents the absorbance (A_λ) of the melted sample normalized by optical path length (l), i.e., $\alpha_\lambda = A_\lambda/l$. The absorbance of the solution is defined as $A_\lambda = \log_{10}(I_0/I)$ at wavelength λ in the case where there is no contribution to light extinction by scattering.

2.3. Absorption Due to Residual and Unknown Chromophores

[17] The sample absorption coefficient (α_λ) at a given wavelength is the sum of the absorption coefficient contributions from all chromophores at that wavelength. For an individual chromophore i the absorption coefficient at each wavelength, $\alpha_{i,\lambda}$, is determined in each snow sample by

$$\alpha_{i,\lambda} = \varepsilon_{i,\lambda}[i] \quad (3)$$

where $\varepsilon_{i,\lambda}$ is the base-10 molar absorptivity of the chromophore at λ, and $[i]$ is the molar concentration of the chromophore in the melted sample. We first determined the contributions of two chromophores – nitrate and hydrogen peroxide – in our snow sample absorption spectra. $\varepsilon_{i,\lambda}$ values for NO_3^- and H_2O_2 were measured both during the campaign in Barrow and post-campaign in the lab in Davis; values agreed well with those published by *Chu and Anastasio* [2003, 2005]. The full set of values (220 to 380 nm) is shown in the supplement (auxiliary Data Set S1 and Figures S2 and S3). As described below, we measured the concentrations of NO_3^- and H_2O_2 in each sample.

[18] For each sample absorption spectrum we determine the "residual" absorption spectrum by subtracting the NO_3^- and H_2O_2 contributions from the total absorption coefficient:

$$\alpha_\lambda(residual) = \alpha_\lambda - \left(\alpha_{NO3-,\lambda} + \alpha_{H2O2,\lambda}\right) \quad (4)$$

This was performed using an IGOR Macro routine. For 24 of our samples we also have data on light absorption by HUmic-LIke Substances (HULIS) (section 2.6). For these samples we subtracted the individual HULIS contribution from the residual light absorption coefficient to determine the amount of light absorption by "unknown" chromophores:

$$\alpha_\lambda(unknown) = \alpha_\lambda(residual) - \alpha_{HULIS,\lambda} \quad (5)$$

For each sample we characterized the total absorption spectrum, residual absorption spectrum, and, if HULIS data was available, the unknown chromophore absorption spectrum. For each of these three spectra for a given sample we summed the absorption coefficients at each integer wavelength to generate a total absorption coefficient (summing over a wavelength range of 220 to 600 nm) and a photochemically active absorption coefficient (summing over a wavelength range of 300 to 450 nm) in order to simplify our results to a single numerical value. These quantities are expressed as $\Sigma\alpha_\lambda$ for total light absorption, $\Sigma\alpha_\lambda$ (residual) for the light absorption due to all chromophores except H_2O_2 and NO_3^-, and $\Sigma\alpha_\lambda$ (unknown) for light absorption due to "unknown" chromophores (i.e., all chromophores except for H_2O_2, NO_3^-, and HULIS).

[19] There is good evidence that a given chromophore has very similar absorption spectra in water and in the ice phase [e.g., *Matykiewiczová et al.*, 2007], and thus our spectra, which were taken on melted snow samples, should be a good surrogate for light absorption in snow. However, some species, such as acids, bases, aldehydes and ketones can undergo transformations in the liquid phase that may result in a shift in their absorption spectra compared to solid solutions or highly concentrated quasi-liquid solutions. For example, small aldehydes can hydrate to form diols in solution. However, the hydration equilibrium is not understood in ice, even for formaldehyde, which is the most abundant aldehyde present in snow [*Houdier et al.*, 2002; *Perrier et al.*, 2002], and whose solid solution with ice has been studied in detail [*Barret et al.*, 2011a]. This is crucial, because diols absorb only below 200 nm, while the C = O bond features an absorption band in the 240–350 nm range [*Liu et al.*, 2009; *Sander et al.*, 2006; *Nemet et al.*, 2004, *Malik and Joens*, 2000; *Sham and Joens*, 1995]. For the small aldehydes HCHO, glyoxal, methylglyoxal, and acetaldehyde, hydration constants K_{hyd} are 10^3, 245, 30, and 1, respectively [*Bell*, 1966; *Henaff*, 1968; *Kurz*, 1967; *Buschmann et al.*, 1982; *Wasa and Musha*, 1970; *Montoya and Mellado*, 1994]; i.e., with the exception of acetaldehyde they are mostly present as diols in solution and will not have any appreciable light absorption in melted snow samples. Even though we do not know which phase they occupy in the snow, we can estimate an upper bound for their potential contribution to light

absorption in unmelted snow samples. The mean concentration of formaldehyde in Barrow snow is 4.1 μg/L [*Barret et al.*, 2011b; Voisin et al., submitted manuscript, 2011]. Assuming an upper bound for the HCHO molar absorptivity (i.e., using molar absorptivities of more strongly absorbing acrolein and methacrolein in their carbonyl forms: 25 and 30 $M^{-1}cm^{-1}$ at 315 and 310 nm, respectively [*Liu et al.*, 2009; *Sham and Joens*, 1995]), HCHO would contribute less than 1% to our observed spectra in the range between 310–315 nm if it was present solely in the carbonyl form in the snow. Similarly, methylglyoxal (with a molar absorptivity for the carbonyl form of 14.7 $M^{-1}cm^{-1}$ at 290 nm [*Nemet et al.*, 2004]) shows a mean concentration in Barrow snow of 0.5 μg/L, and would add only 0.02% to the measured absorption at 290 nm if it was present in the carbonyl form in the snow. Thus, we expect there are only small differences in light absorption by soluble chromophores between the unmelted and melted states of the same snow.

2.4. Analysis for H_2O_2

[20] We analyzed one aliquot from each snow sample for H_2O_2 using HPLC separation (Inertsil® ODS-2 analytical column with guard column) with post-column derivatization with *p*-hydroxyphenylacetic acid in an enzymatic reaction to form a fluorescent dimer [*Kok et al.*, 1995], and detection by a Shimadzu RF-551 spectrofluorometric detector. Calibrations were performed with a series of freshly made, dilute H_2O_2 solutions generated from 30% H_2O_2 (Fisher, certified A.C.S.) that was verified by UV-vis absorbance (using ε_{H2O2} = 37.9 M^{-1} cm^{-1} at 240 nm [*Chu and Anastasio*, 2005]). The resulting 3σ detection limit for H_2O_2 with the HPLC method was 75 nM. To estimate H_2O_2 loss in our sample aliquots during storage, we analyzed a series of H_2O_2 standards by LWCC UV-vis in Barrow, froze and stored them, and then analyzed them for H_2O_2 in Davis as part of the snow sample aliquot analysis. We found that H_2O_2 in the frozen standards decayed with a rate constant of -0.046% d^{-1}. We then used this decay constant to adjust the H_2O_2 concentration that we measured in Davis to the H_2O_2 concentration expected on the day that the snow sample absorption spectrum was measured in Barrow. The average correction was 7.7% of the measured H_2O_2 value, with the correction for any given sample depending on the period that it remained in frozen storage.

2.5. Ion Chromatography

[21] An aliquot for each snow sample was also analyzed for anions using ion chromatography (Dionex IC DX120, with Dionex AS14 column and, AG 14 guard column, and Anion Atlas Electrolytic Suppressor). Calibrations were carried out using a multicomponent certified anion standard (AllTech Mix A) for F^-, Cl^-, Br^-, NO_2^-, NO_3^-, PO_4^- and SO_4^-, and a series of diluted NO_3^- solutions made from solid $NaNO_3$ (Fisher, certified A.C.S.). The resulting 3σ detection limit for NO_3^- was 0.77 μM. Similarly to H_2O_2, nitrate standards were analyzed in Barrow, frozen, and then re-analyzed in the lab in Davis. No decay or alterations of these samples were detected during freezing and transport.

2.6. HULIS

[22] For a subset of 24 of our snow samples, we also extracted polyacidic HUmic-LIke Substances (HULIS) from parallel, collocated melted snow samples; this HULIS was analyzed for their light absorption spectra and total organic carbon (TOC) concentrations (Voisin et al., submitted manuscript, 2011). We used HULIS data from each sample to determine the contribution of HULIS toward light absorption in the collocated sample that we analyzed for light absorption. The average TOC concentration was 6.5 μg-C/L-melted snow. The HULIS light absorption coefficient at 300 nm in our samples is typically 0.015 m^{-1}; the average mass- and molar-normalized absorption coefficients for HULIS are shown in auxiliary material Figure S4. HULIS absorption measurements below 240 nm have large uncertainties because of TOC blank corrections. The median relative error of the absorption spectra varied between 10–20% at 300 nm and 30–45% at 450 nm.

[23] While *Graber and Rudich* [2006] point out that the term "HULIS" is defined for atmospheric samples, and has properties that are different from terrestrial and aquatic humic and fulvic substances, we use the term HULIS here more broadly to include atmospheric-derived HULIS as well as soil/marine humics and fulvic materials. We use "HULIS" (as opposed to "humics," for example) because (a) the extraction protocol used by Voisin et al. (submitted manuscript, 2011) was optimized for HULIS, but not humics, and (b) the HULIS material at Barrow has not been processed sufficiently to fall into the humics category, being derived either by direct infusion of plants, or from exopolymer saccharides (EPS or EPS-like) material from the ocean. More details on the HULIS results and its nature are provided by Voisin et al. (submitted manuscript, 2011).

[24] Thirty-four of the HULIS samples were taken close to the snow samples measured for light absorption described in this paper: 4 samples were identical, 14 samples were taken from the same snow at the same time, and another 6 samples were taken from the same snow within 30 min of the light absorption sample. The individual light absorption in these 24 HULIS samples can be confidently compared to our light absorption spectra on the whole snow sample (see below). Further 10 HULIS spectra were taken from snows not in the immediate vicinity (location or time) of our light absorption samples. These HULIS sample spectra show larger absorption than our snow light absorption spectra (up to 800%, this is further discussed by Voisin et al. (submitted manuscript, 2011)). We therefore include only the collocated 24 HULIS samples in our further analysis.

2.7. Sunlight Absorption

[25] Multiplying our measured absorption coefficients by the actinic flux is approximately equal to the rate of sunlight absorption in the melted snow [*Anastasio and Robles*, 2007]:

$$\textit{Total rate of sunlight absorption} \approx \sum\nolimits_{\lambda}(I_\lambda \times a_\lambda) \qquad (6)$$

where I_λ is the actinic flux (photons cm^{-2} s^{-1} nm^{-1}) measured at Barrow during our campaign.

3. Results and Discussion

3.1. Typical Light Absorption Spectra for Barrow Snows

[26] The majority of our snow samples showed an absorption spectrum as in Figure 1, with α_λ values of 0.1 to

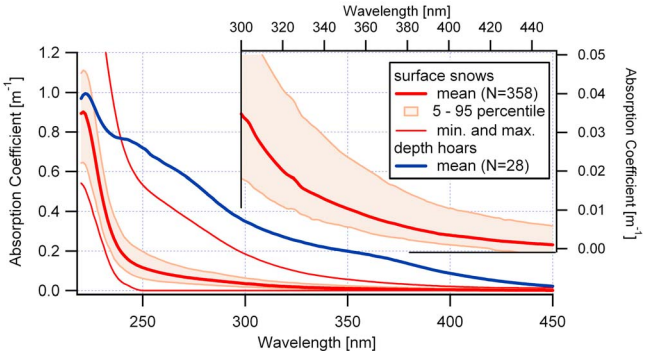

Figure 2. Mean absorption spectra of terrestrial surface snows (upper 5 cm of snowpack) at Barrow during our campaign (thick red line). The pink shaded area encompasses the absorption spectra for 90% of our surface snow spectra (with the upper and lower pink lines representing samples at the 5th - and 95th percentiles of all the data). The thin red lines show the minimum and maximum spectra. The insert shows a detailed view between 300 and 450 nm for these 90% of our terrestrial surface snow samples. The blue line in the main graph shows the mean absorbance spectrum for terrestrial depth hoar and indurated depth hoar samples.

0.15 m^{-1} at 250 nm. The general appearance of our spectra is similar to those shown by *Anastasio and Robles* [2007], although our spectra are smoother because of better instrumentation and averaging of replicate analyses.

[27] Figure 2 shows the range of light absorption spectra we observed for the 358 surface snow samples taken from the upper 5 cm of the snowpack during our campaign. The mean light absorption coefficient of these samples at 300 nm (i.e., α_{300}) is 0.034 m^{-1}. In contrast, the largest absorption coefficients in our terrestrial snow spectra are seen in samples of (indurated) depth hoar, where the mean value of α_{300} is an order of magnitude higher, at 0.36 m^{-1} (Figure 2). This more absorptive snow layer was closest to the ground, contained significant amounts of vegetative debris, had a yellowish color when melted, and contained significant amounts of HULIS (see below). Our Barrow surface snow samples have higher absorption coefficients than surface snow samples from Summit, Greenland, and Dome C, Antarctica, where average light absorption coefficients at 280 nm were 0.014 m^{-1} and 0.007 m^{-1}, respectively [*Anastasio and Robles*, 2007].

3.2. Contributions of Nitrate, Hydrogen Peroxide, and HULIS to Light Absorption

[28] For each snow spectrum we subtracted the light absorption by H_2O_2 and NO_3^- (equation (4)), as illustrated in Figure 3. The median NO_3^- concentration in our Barrow surface snow samples was 3.7 μM (Table 1), with 85% of the values below 5 μM. NO_3^- concentrations were distributed fairly uniformly, i.e., they showed no systematic variation with snow type or layers for terrestrial snows. There is some evidence that NO_3^- decreased with depth in the buried snow layers (possibly due to aging and the associated snow metamorphism), however, this is not statistically significant (data not shown). In all samples, however, the contribution of NO_3^- absorbance to the observed spectra was significant only below approximately 245 nm; at longer wavelengths the median contribution from NO_3^- was highest at 309 nm, where nitrate accounted for 9% of light absorption.

[29] For hydrogen peroxide the median concentration was 0.18 μM, while 85% of the values were below 1 μM (Table 1). H_2O_2 was not distributed evenly in the snow, with surface layers showing significantly higher concentrations than buried layers, due to exchange processes between the snow surface and the overlying atmosphere and chemical reactions in the snow surface layers (Domine et al., submitted manuscript, 2011b). As illustrated in Figure 3, hydrogen peroxide made an insignificant contribution to light absorption in our Barrow snow samples, with the maximum H_2O_2

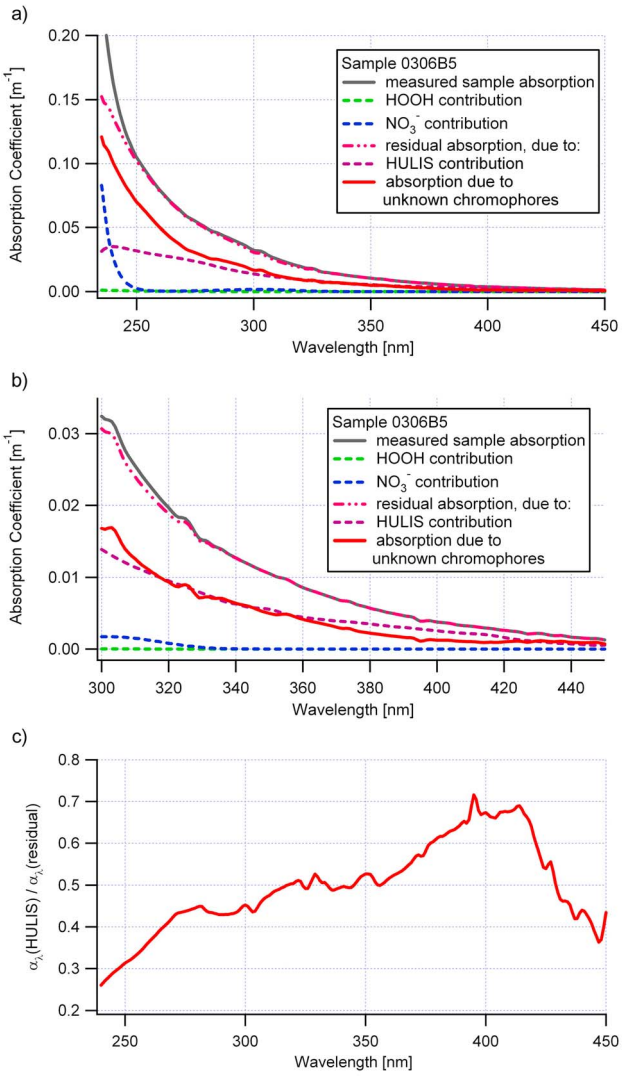

Figure 3. Example of subtracting absorption contributions from known chromophores from a measured snow absorption spectrum over (a) most of the wavelength range (240–450 nm) and (b) the photochemically relevant wavelength range (300–450 nm). H_2O_2 is not a significant contributor to the absorption spectrum of Barrow snow (green dashed line). The NO_3^- contribution is significant only below ca. 245 nm (blue dashed line). (c) The HULIS contribution to the residual absorption coefficient varies with wavelength.

Table 1. Measured Concentrations of Known Chromophores H_2O_2 and NO_3^- [μM] in Terrestrial Barrow Snow Samples

	H_2O_2	NO_3^-
Number of cases	466	455
Minimum	not detected	not detected
Maximum	9.56	17.82
Median	0.18	3.70
Mean	0.53	3.70
95% CI Upper	0.62	3.87
95% CI Lower	0.44	3.54
Standard Dev	0.96	1.76

contribution of 0.34% (median value) at 245 nm; at wavelengths above 300 nm, the median H_2O_2 contribution was less than 2.2%. In comparison, at Summit and Dome C, Antarctica H_2O_2 contributed up to 19% and 15%, respectively, to the measured absorption coefficients above 300 nm [*Anastasio and Robles*, 2007]. Although H_2O_2 is a negligible contributor to light absorption in snow at Barrow, it is still a major photochemical source of the highly reactive hydroxyl radical at Barrow (France et al., submitted manuscript, 2011), as it is at other polar sites [*Beine and Anastasio*, 2011; *Chu and Anastasio*, 2005; *Thomas et al.*, 2010]. More details on H_2O_2 concentrations and behavior in our Barrow samples are given by Domine et al. (submitted manuscript, 2011b).

[30] Figures 3a and 3b illustrates that subtracting the minor contributions of H_2O_2 and NO_3^- from the measured absorption coefficients results in the "residual absorption coefficient" (equation (4)). This α_λ (residual) accounts typically for 95% of the absorption in the photochemically relevant spectral range from 300–450 nm. This is overall a significantly larger fraction than observed in either Summit or Dome C snow samples, where chromophores other than H_2O_2 and NO_3^- contributed, on average, 60% and 53%, respectively, of light absorption in the sunlight region [*Anastasio and Robles*, 2007]. We find no correlation between the residual light absorption and either NO_3^- or H_2O_2 in Barrow surface snows, suggesting that the sources of the residual snowpack chromophores are different from those of nitrate and hydrogen peroxide.

[31] We also determined the contributions of HULIS to light absorption in a subset of our snow samples. Polyacidic HULIS are the major organic constituents of soils, peat, dystrophic lakes, and ocean water; they are a complex mixture of many different acids containing carboxyl and phenolate groups, and resemble terrestrial and aquatic humic and fulvic acids. For these 24 samples, the average HULIS carbon concentration was 6.5 μg C/L-melted snow (Voisin et al., submitted manuscript, 2011). As shown in auxiliary material Data Set S1 and Figure S4, the average light absorption spectrum of our snow HULIS samples show significant absorption throughout the observed UV and visible range. For each of the 24 samples where we have HULIS data, we subtracted the absorption coefficient due to HULIS in that sample from the residual absorption coefficient at the same wavelength. As shown in Figure 3c, HULIS is a major component of light absorption at all wavelengths above 240 nm and is a dominant component for actinic wavelengths absorbed by our samples. The HULIS contribution generally increases steadily with increasing wavelength over the observed spectral range; for example, as shown in Figure 3c, it grows between approximately 25% at 240 nm to about 70% at 400 nm.

[32] Subtracting the HULIS, NO_3^-, and H_2O_2 contributions from a given sample absorption spectrum leaves us with the contribution due to "unknown" chromophores (equation (5)). As shown in Figure 4, light absorption due to the unknown chromophores exhibits the same general behavior as the overall sample light absorption: a relatively smooth, featureless curve that decays approximately exponentially from shorter to longer wavelengths. Figure 4 also shows that, within the method uncertainties, the average value of α_λ (unknown) is essentially 0 above 350 nm; i.e., HULIS can account for most of light absorption at wavelengths above 350 nm, while the unknown chromophores have only minor absorption in this range.

[33] Figure 5 shows a statistical summary of the contributions of H_2O_2, NO_3^-, HULIS, and unknown chromophores to the summed light absorption coefficients, $\Sigma\alpha_\lambda$, in our snow samples (see section 2.3 for the definition of $\Sigma\alpha_\lambda$). Figures 5a and 5c show results for the entire set of 350 surface snow samples, while Figures 5b and 5d show results for the subset of 24 snow samples with HULIS data.

[34] In 350 terrestrial surface snow samples H_2O_2 and NO_3^- contribute a median of 0.1% and 51%, respectively, to the total absorption in the full spectral range from 220–600 nm (Figure 5a), and 0.02% and 4.9% to the total absorption in the photochemically relevant range from 300–450 nm (Figure 5c). The samples that show higher NO_3^- contributions, are snows with smaller total light absorption between 300–310 nm. As shown in Figure 5b, the HULIS contribution is sizable across the UV-vis spectral range. The median HULIS contributions to total light absorption are 18% for the complete spectral range (220–600 nm) and 48% for the spectral range of interest for photochemistry (300–450 nm) (Figure 5d). Unknown chromophores are the other major contributor to light absorption in the 300–450 nm range, typically accounting for 47% of $\Sigma\alpha_\lambda$ in our surface snow samples.

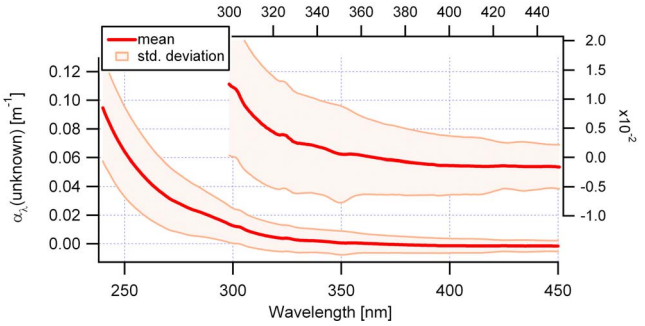

Figure 4. Mean (and standard deviation) of the absorption coefficients from unknown chromophores for the 24 samples with HULIS data. Recall that light absorption coefficients for unknown chromophores are determined by subtracting the HULIS contribution from the residual absorption coefficients (equation (5)). $\alpha_{\lambda\ (\mathrm{unknown})}$ is essentially zero (within the method uncertainties) above 350 nm.

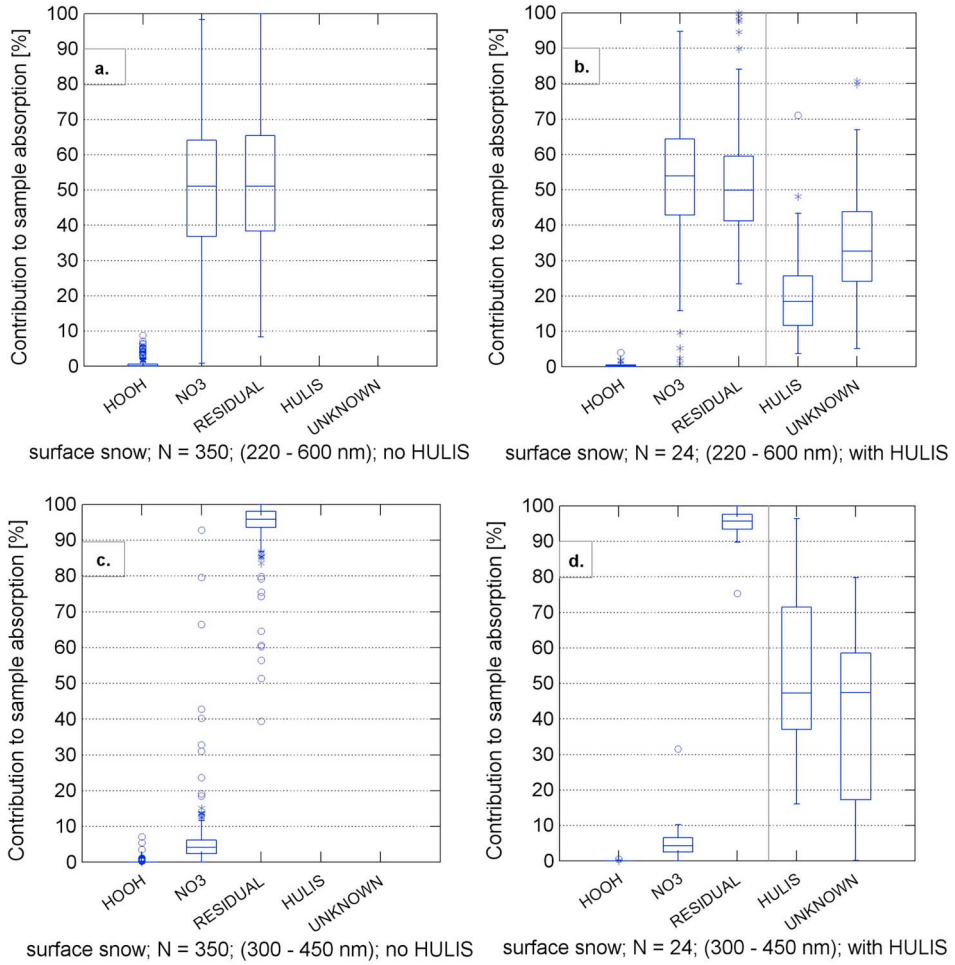

Figure 5. Box-and-whisker plots of the contribution of different chromophores to the overall sample absorption coefficients. The center horizontal line marks the median of the sample, while the length of each box shows the central 50% of the values (i.e., the bottom and top of each box ("hinges") are the first and third quartiles). The whiskers show the range of values that fall within the inner fences (e.g., inner upper fence = upper hinge + 1.5 × interquartile range). Values between the inner and outer fences are plotted with asterisks (outer upper fence = upper hinge + 3 × interquartile range). Values outside the outer fence are plotted with circles [*SPSS, Inc.*, 1999]. (a) Contributions to the summed absorption coefficients over the full spectral range (220–600 nm) for all terrestrial surface snow samples. H_2O_2 and NO_3^- contribute a median of 0.1% and 51% of the total absorption, while residual species (i.e., HULIS and unknown chromophores) together contribute a median value of 52%. (b) Contributions to absorption over the full spectral range (220–600 nm) for the 24 surface snow samples for which we have HULIS data. The dashed vertical line indicates that the HULIS and unknown fractions are part of the residual absorbance. The median fraction of HULIS absorbance in surface samples is 18.5% and the median remaining fraction due to unknown chromophores is 32.6%. (c) Contributions to absorption in the photochemically active spectral range (300–450 nm) for all surface snow samples. H_2O_2 and NO_3^- contribute a median absorbance of 0.02 and 4.9%, while the residual contributes a median value of 94.8%. (d) Contributions to absorption in the 300–450 nm range for the 24 surface samples with HULIS data. The dashed vertical line indicates that the HULIS and unknown fractions are part of the residual absorbance. HULIS contributed between 16 and 89% to the sample absorption, with a median value of 47%, while the median contributions from nitrate and hydrogen peroxide were 0.02 and 4.9%, respectively. The remaining 48% of absorption is due to unknown chromophores.

3.3. Potential Contribution of Nitrite to Light Absorption

[35] We also estimated the potential contribution of nitrite to light absorption in the snow, since NO_2^- has been found in polar snows [*Li*, 1993; *Amoroso et al.*, 2010] and has reasonably high molar absorptivities in the UV range [*Chu and Anastasio*, 2007]. While NO_2^- is only one form of N(III), which consists of NO_2^-, HONO, and H_2ONO^+, it should be the dominant form in our melted samples: we estimate the

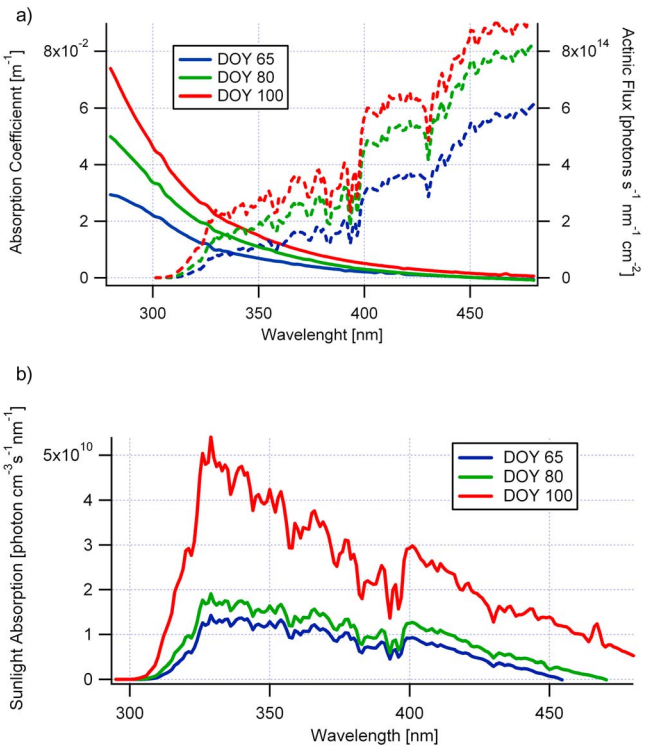

Figure 6. (a) Light absorption spectra for 3 surface samples (all fresh blowing snow) on DOY 65, 80, and 100 (solid lines, left axis). These 3 examples span the typical range of absorption during the campaign. The right axis shows the spectral actinic fluxes for each sample date measured at solar noon (3m above the snow surface). (b) Rates of sunlight absorption for the snowpack on DOY 65, 80, and 100, the calculation followed the approach of *Anastasio and Robles* [2007]. These curves show one of lowest (blue curve for DOY 65 evening) and one of the highest rates (red curve) of sunlight absorption for typical surface snow samples during our campaign.

average pH of our melted snow samples to be above pH 5, while the pK_a for HONO is 2.8 [*Chu and Anastasio*, 2007]. During the campaign at Barrow NO_2^- in melted snow was measured for a small subset of samples (Villena et al., submitted manuscript, 2011), with a resulting mean concentration of 22 nM. This concentration corresponds to a value of $\Sigma\alpha_\lambda$ (NO_2^-) over the 300–450 nm range of 4.5×10^{-5} m^{-1}, which would only account for 0.003% of the average surface snow value of $\Sigma\alpha_\lambda$ (residual), 1.4 m^{-1}, in that spectral range.

3.4. Sunlight Absorption by Surface Snows

[36] The sum of residual absorption $\Sigma\alpha_\lambda$ (residual) in bins between 250–275, 275–300, 300–325, 325–350, 350–375, and 375–400 nm contribute on average 11.9, 6.7, 3.4, 1.9, 1.2, and 0.7% to the total $\Sigma\alpha_\lambda$ (residual) between 220–600 nm, and fractions of a percent at longer wavelengths. However, solar actinic flux is zero below 300 nm, so that photochemical activity and production arises from components that contribute on average only 7.5% to the total measured absorption.

[37] The effect that this small percentage of chromophores has on photochemistry during our campaign can be quantified by calculating the sunlight absorption of our surface snows (equation (6)). As Figures 6a and 6b show, the midday actinic flux increased over the course of our campaign, and the actual solar radiation absorbed by our snow samples varied greatly, even though the measured absorption of our samples varied only slightly during our campaign (see below). As the season progressed the total rate of sunlight absorption at the snow surface increased significantly from approximately 1.1×10^{12} [photons cm^{-3} s^{-1}] in the spectral range from 300–450 nm on DOY 65 to 1.5 and 3.9×10^{12} [photons cm^{-3} s^{-1}] on DOY 80 and 100, respectively. The total sunlight absorption at Summit, Greenland at the end of May [*Anastasio and Robles*; 2007] was 1–4 $\times 10^{11}$ [photons cm^{-3} s^{-1}], which is an order of magnitude less than at Barrow. The maximum actinic flux shown by *Anastasio and Robles* [2007] was 5×10^{14} [photons cm^{-2} s^{-1} nm] at 365 nm, which is about 40% higher than our results for DOY 100 (3.4×10^{14} [photons cm^{-2} s^{-1} nm] at 365 nm). However, our mean absorption coefficients are more than double the values at Summit; further, their assumption that there was no absorption at wavelengths longer than approximately 400 nm leads to an underestimation of sunlight absorption. For example, Figure 6b shows that a significant fraction of sunlight absorption in our Barrow samples is occurring in the visible wavelengths above 400 nm.

3.5. Potential Sources of Chromophores

[38] Our snow samples were taken daily from a range of depths to explore the stratigraphy and temporal evolution of the snowpack. Both can lead to important insights about the sources of chromophores in the snowpack. Most of our samples were taken from the upper 20 cm of the snowpack. The very surface layer consisted either of a thin layer (<5 mm) of diamond dust and surface hoar during calm periods, or of a discontinuous layer of soft, wind-drifted snow, during and just after windy episodes (Domine et al., submitted manuscript, 2011b). Below that was a hard wind-packed layer, up to 20 cm thick, in places topped by a thin (<2 mm) melt-freeze crust. Bottom layers were faceted crystals and depth hoar of various types (soft, columnar and/or indurated) (Domine et al., submitted manuscript, 2011a). In those surface or near surface samples the surface layers generally show slightly higher $\Sigma\alpha_\lambda$ (residual, 300–450 nm) than the deeper layers, though not as clearly defined as in the case of H_2O_2. As in the case of H_2O_2, $\Sigma\alpha_\lambda$ (residual) in the snow surface is influenced by atmospheric deposition and other atmosphere – snow exchange processes. Further, the deposition of diamond dust and the growth of surface hoar modify the surface continually (Domine et al., submitted manuscript, 2011b). The very surface consisting of surface hoar and diamond dust shows a median $\Sigma\alpha_\lambda$ (residual) between 300 and 450 nm of 1.25 m^{-1}, while the melt-freeze crust immediately below has values approximately 25% lower. At depths around 8 cm $\Sigma\alpha_\lambda$ (residual) drops further to about 0.8 m^{-1}.

[39] To further explore this depth dependence, on DOY 63 we participated in a more detailed survey that focused on vertical and horizontal physical changes in the snowpack (Domine et al., submitted manuscript, 2011a). Figure 7 shows that the lower layers of the pack exhibit significantly higher $\Sigma\alpha_\lambda$ (residual), with values up to 33 m^{-1}. The

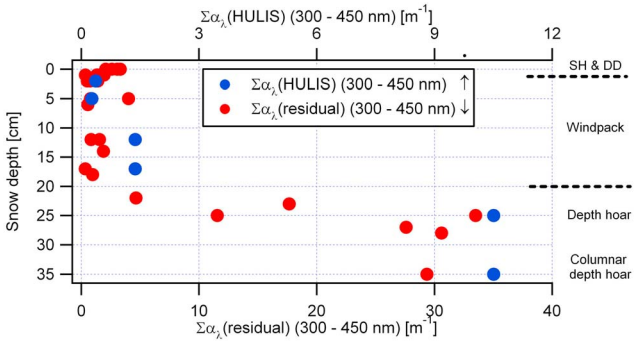

Figure 7. Depth profile of $\Sigma\alpha_\lambda$ (residual) (300–450 nm) on DOY 63. As discussed by Domine et al. (submitted manuscript, 2011a) the snow layers were: surface hoar (top 0.5 cm), surface wind pack, wind pack (variable depth, typically to about 20 cm), (indurated) depth hoar (20–30 cm), columnar depth hoar containing visible vegetative debris (below about 25 cm). The blue symbols (top axis) show the summed absorption coefficients from HULIS, $\Sigma\alpha_\lambda$ (HULIS), in six collocated snow samples.

lowest layers, columnar depth hoar at 40 cm, were mixed in with vegetation and vegetative debris. As mentioned above, the melted samples had a yellowish appearance, indicative of HULIS and other organic material. The influence of these terrestrial sources of organic material extended only through the depth hoar layers below approximately 22 cm; the upper snow layers are much less influenced by this source.

[40] Processes that shape the snowpack include precipitation, wind, and the temperature gradient in the snowpack (Domine et al., submitted manuscript, 2011a). The weather is windy most of the time at Barrow. Recent snowfalls are raised by wind, the grains rounded by sublimation, and the snow is most of the time re-deposited in discontinuous layers, so that 2 neighboring stratigraphic profiles may sample different snowfalls or wind drifts. The transitions between layers are usually clearly defined, and only a small mixed zone is seen. Diamond dust, surface hoar and snow falls contribute to the growth of the snowpack throughout the season. The layering of the snowpack is clearly observed in the snow profile in Figure 7; this layering separates the land surface, which is clearly a source for vegetation-derived organic material, from the upper snow layers. Throughout the windpack that appears homogeneous, but is composed of many precipitation and wind events, the $\Sigma\alpha_\lambda$ (residual) is fairly low.

[41] During the depth survey on DOY 63 we also saw evidence that there is a marine source of chromophores. Snow samples with high $\Sigma\alpha_\lambda$ (residual) values also showed elevated Cl^- ion content (Figure 8). This survey is the only occasion where such a relationship was present for inland snows; most surface hoar and windpack showed no correlation at all with Cl^-. Our sampling site was within a few km of the coast both to the North and West of Barrow. Cl^- may thus be used as a tracer of marine influence and sea-salt aerosols that impacted our sampling site. The marine sources can be estimated from the insert in Figure 8, which shows the $\Sigma\alpha_\lambda$ (residual) – Cl^- correlation for different marine-derived snow, ice, brine, and frost-flower samples taken on DOY 79 (Beine et al., submitted manuscript, 2011; Douglas et al., submitted manuscript, 2011). The correlation is statistically significant. However, even though the $\Sigma\alpha_\lambda$ (residual) values are the highest seen during our campaign, the slope with Cl^- is very small, because marine Cl^- is even larger.

[42] Since we do not observe the marine $\Sigma\alpha_\lambda$ (residual)/Cl^- slope of 2.1×10^{-5} $m^{-1}/\mu M$ Cl^- in our depth profile, but a value that is 4 orders of magnitude larger (0.014 $m^{-1}/\mu M$ Cl^-; Figure 8 and auxiliary material Figure S5) we likely observe a mixture of both marine and terrestrial/floral sources of chromophores. Because of enhanced Cl^- values, a possible $\Sigma\alpha_\lambda$ (residual)/Cl^- correlation, and the very high absorbance values that we observed in frost flowers we cannot exclude the possibility that even the layers that are close to vegetation might be influenced by marine sources during their formation, unless there is a terrestrial source of Cl^-. Additionally, both Br^- and SO_4^{2-} increase significantly in concentration between the top 0–20 and the 20–40 cm deep layers (Br^-: 0–0.5 μM versus 1–2 μM; SO_4^{2-}: 0–10 μM versus 20–45 μM) on DOY 63, which, again, is indicative of the marine influence in the these lower layers.

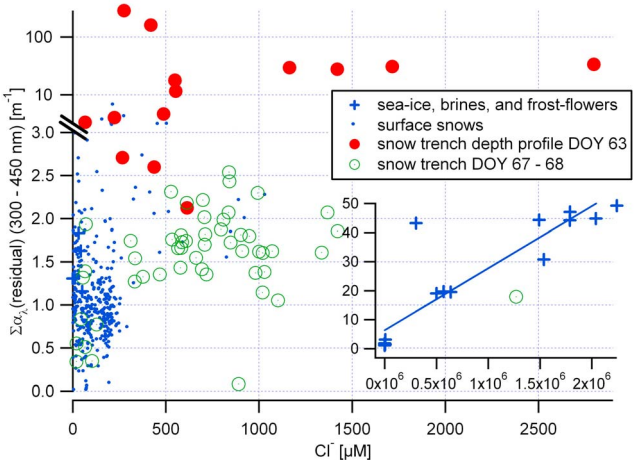

Figure 8. Relationship of $\Sigma\alpha_\lambda$ (residual) with Cl^- in different snows. Note that the y axis is split: it is linear between 0 and 3 [m^{-1}], and logarithmic above, showing the range from 3.1 to 240. The insert shows the correlation of $\Sigma\alpha_\lambda$ (residual) (300–450 nm) versus Cl^- concentration for fresh and old sea-ice, brine, snow on sea-ice, and frost flowers samples taken on DOY 79 (blue crosses) (Douglas et al., submitted manuscript, 2011). The slope is 2.13×10^{-5} ($\pm$ 2.6×10^{-6}) [$m^{-1}/\mu M$ Cl^-], (intercept 6.4 $\pm$ 3.2, R^2 = 0.817, N = 17, p = 0.0000). Most surface snow samples (blue dots) show no correlation. On DOY 63 a depth survey was performed (red circles); both Cl^- and $\Sigma\alpha_\lambda$ values exceed the normal surface snow range significantly (see Figure 7); there may be a linear correlation (see auxiliary material Figure S5). The slope is 0.014 [$m^{-1}/\mu M$ Cl^-]. In the days after the survey, snowfalls and winds deposited fresh snow in the open trench and partly obliterated the break in the snow surface. Green circles show samples taken from the trench during those days. The Cl^- values are higher than in surface snows, as high as in trench when it was fresh; but the $\Sigma\alpha_\lambda$ values have dropped by about an order of magnitude.

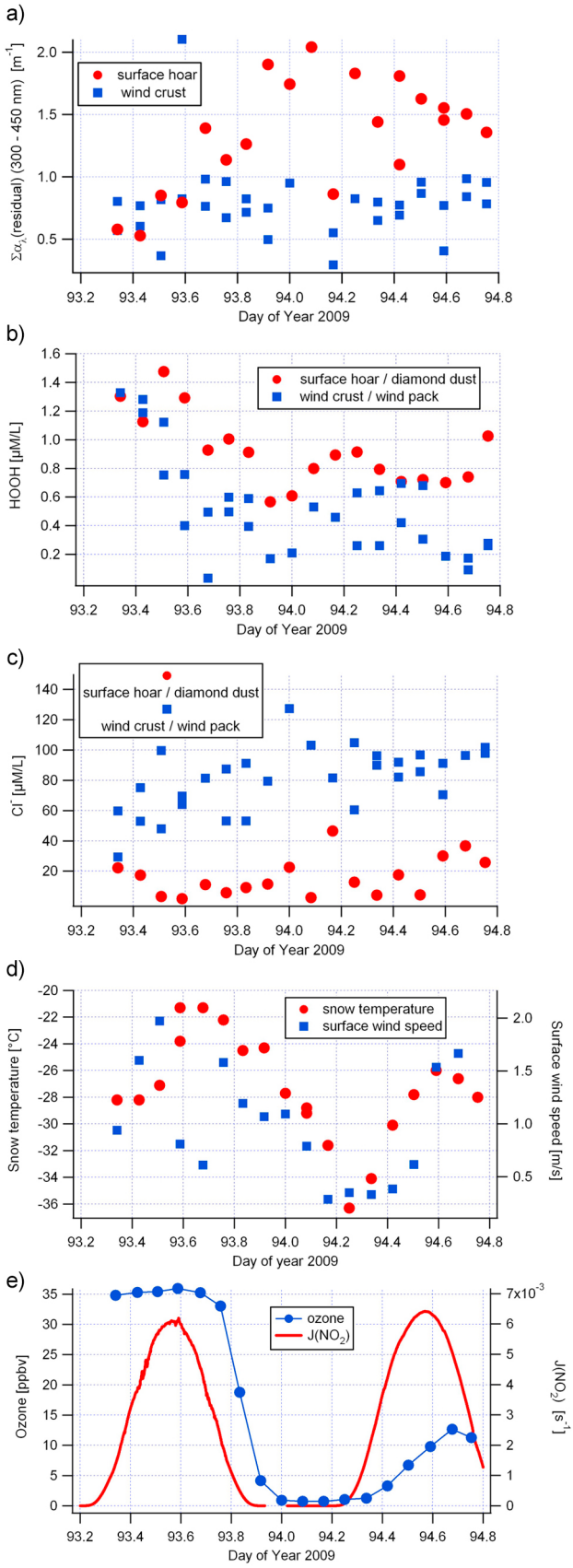

[43] Thus, in autumn, when the snowpack is thin, the discontinuous character of the snow layers likely implies that patches of tundra remain exposed to wind action, providing a source of vegetal and terrigeneous material to the snow. The unfrozen sea or thin sea ice, also exposed to wind, will provide sea-salt aerosol to the inland snow. We therefore expect that the depth hoar layers, which form in autumn are enriched in vegetal, terrigenous and sea salt elements. Eventually, all the continental area is snow covered, as we observed in late February, so that input of ground material essentially stops. Likewise, input of sea salt was reduced by the near complete sea ice cover. The sea salt source did not stop completely, however, because of the lead that frequently opens off of Barrow, and because snow on sea ice can be a source of sea salt. In late winter and spring, additional sources of impurities to the snow may become important. These include Arctic Haze deposition and halogen chemistry during ozone depletion events that may oxidize organic compounds, leading to the formation of organic aerosols.

3.6. The 36-h Experiment

[44] Snow samples are discrete samples, so that with only three or four sampling times per day diurnal and shorter term variations can often be missed. On April 3 and 4, 2009 (DOY 93 - 94) we sampled snow every 2 h for a 36-h period to explore short-term variations in the snow. For additional aspects of this 36-h experiment see H. W. Jacobi et al. (Chemical composition of the snowpack during the OASIS 1 spring campaign 2009 at Barrow, Alaska, submitted to *Journal of Geophysical Research*, 2011).

[45] Figure 9 shows time series of $\Sigma\alpha_\lambda$ (residual) (300–450 nm), and other measured parameters during this experiment; different symbols identify surface hoar/diamond dust as surface layer, and the surface melt-freeze crust and the homogeneous windpack as sub-surface layers. Both $\Sigma\alpha_\lambda$ (residual) in the spectral range from 300 to 450 nm and the ratio of this value to the entire spectral range from 220 to 600 nm in the surface layers show a variation over the course of this experiment, with maxima right after midnight; however, the variation is likely not diurnal. The snow surface temperature (Domine et al., submitted manuscript, 2011a) shows an opposite cycle, however; the correlation between $\Sigma\alpha_\lambda$ (residual) and temperature is not statistically significant and the peaks of the maxima did not occur at the same time. The minima in snow temperature and surface wind speed occurred right around sunrise. The surface H_2O_2 concentration seems to be modulated foremost by the surface winds,

Figure 9. Time series of residual light absorption (300–450 nm) during the 36-h experiment. (a) Surface samples (surface hoar and diamond dust) are shown as red circles, while sub- surface samples (surface wind crust and below) are shown as blue squares. (b) Time series of H_2O_2 concentrations in the surface (red) and sub-surface (blue) layers. (c) Time series of Cl^- concentrations in the surface (red) and sub-surface (blue) layers. (d) Snow surface temperature [°C] (left axis, red symbols); Wind speed at 60 cm above snow surface (right axis, blue symbols). (e) Ozone (left axis, blue symbols) and $J(NO_2)$ for the experiment, as a proxy for the incident actinic flux (right axis, red line).

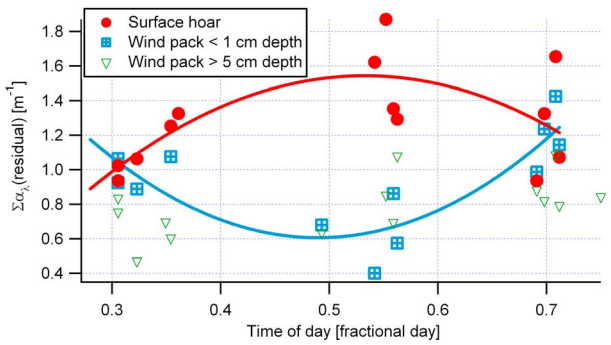

Figure 10. Diurnal profile of $\Sigma\alpha_\lambda$ (residual) (DOY 80.0–84.0, 300–450 nm) in surface hoar, (red circles) and the wind pack immediately below that layer (blue squares). Lower layers of the wind pack (green triangles) show no diurnal variation.

and shows a secondary maximum right at the coldest temperatures, consistent with atmosphere – surface exchanges [e.g., *Hutterli et al.*, 2001]. As discussed above, marine influences are mostly seen in deeper snow layers, and not on the surface. Both Cl^- and SO_4^{2-} show lower values on the surface, and confirm this general finding also for this 36-h period.

[46] The 36-h experiment included an ozone depletion period. The drop in O_3 to near zero was associated with the highest values of $\Sigma\alpha_\lambda$ (residual) between 300–450 nm in the surface hoar (but not in the wind crust) (Figure 9) as well as slightly higher values of $\Sigma\alpha_\lambda$ (residual) in the range below 300 nm (not shown). An effect of O_3 on the chromophores is visible occasionally during individual periods, however, it does not hold for the entire campaign or all surface snows. O_3 and its depletion does have some effect on the absorption below 250 nm at some times; this is not connected to NO_3^-. It is conceivable that halogen chemistry oxidizes organics in the snow to form chromophores that absorb more strongly. However, the data scatter during these periods makes it difficult to identify causal relationships.

[47] Atmospheric HONO data for this period (not shown) are available starting at midnight of April 4 (DOY 94.0) (Villena et al., submitted manuscript, 2011). HONO was unusually high, around 450 pptv, between DOY 94.06–94.13, either due to local pollution or coinciding with the observed O_3 depletion. It is conceivable that atmospheric HONO deposits during this period onto the surface snow and causes the observed peak in $\Sigma\alpha_\lambda$ (residual). However, we do not detect significant changes in $\Sigma\alpha_\lambda$ (residual) at the wavelengths of the maximum NO_2^- absorption (372 nm,) compared to spectral regions where NO_2^- does not absorb, between before and after the increased HONO concentrations. Since the NO_2^- contribution to $\Sigma\alpha_\lambda$ (residual) is very small (see 4.3 above) it is still possible that (organic) co-pollutants present in the air mass deposit onto the snow surface and cause an increase in $\Sigma\alpha_\lambda$ (residual).

[48] In summary, the residual absorption $\Sigma\alpha_\lambda$ (residual) responded to both temperatures and winds, but we do not see a response to incident light. Similar to H_2O_2 the response occurs mostly at the very surface, while the deeper melt-freeze crust and sub-surface layers show stable levels of absorption coefficients throughout the period. $\Sigma\alpha_\lambda$ (residual) thus probably contains some smaller, volatile compounds that are affected by temperature and winds but that do not photolyze readily.

3.7. Diurnal Variations

[49] Diurnal variations in the absorption coefficients were previously reported for Summit [*Anastasio and Robles*; 2007], with a dip in $\Sigma\alpha_\lambda$ in the surface layers observed around noon on one day. A similar behavior might be inferred from our surface samples in the beginning of April during the 36-h experiment (see section 3.6), but the signal is not very clear. At no other time during the campaign did we sample at night. For the most part of our campaign we see no diurnal behavior in light absorption coefficients (see for example auxiliary material Figure S6) for more than one day except for one further period (DOY 80.0–84.0), which is shown in Figure 10. During this period we observed a mid-day maximum of approximately 1.5 m^{-1} in the surface hoar and diamond dust on the very top of the snowpack, while the wind-drifted snow immediately below shows a mid-day minimum in $\Sigma\alpha_\lambda$ (residual) of 0.6 m^{-1}. This is consistent with the observations by *Anastasio and Robles* [2007] for the wind-drifted snow layer, as these authors removed the surface hoar before sampling. For our Barrow snow, both the surface hoar and surface wind pack show similar $\Sigma\alpha_\lambda$ (residual) values in the morning and evening, but different behavior near midday, suggesting that chromophores are exchanged between these surface layers. Deeper snow layers show no consistent, statistically significant behavior, and it is thus unknown whether this exchange extends further into the snowpack. The mean spectral α_λ (residual) of the difference between mid-day maxima in the surface layer and the minimum in the wind-drifted snow below is broad and featureless and resembles very much the rest of our absorption spectra (auxiliary material Figure S7). It thus gives little evidence on the chemical nature of the species that are exchanged.

3.8. Photo-bleaching of Snow Chromophores

[50] The sum of residual absorption $\Sigma\alpha_\lambda$ (residual) between 300 and 450 nm in surface snows (top 5 cm) declines over the duration of our campaign, indicating a loss of photoactive material, likely due to photochemical reactions ("photo-bleaching") (Figure 11). For the entire time period a slope of −0.015 m^{-1}/day (relative standard error 0.0034, p = 0.00003) is statistically significant. The effective ambient lifetimes (considering both chemical and physical processes) of the chromophores that account for $\Sigma\alpha_\lambda$ (residual) are apparently relatively long, as their decline is small. However, stronger day-to-day modulations of $\Sigma\alpha_\lambda$ (residual) are caused by winds and snowfall. At Barrow periods of no or calm winds alternated with stronger winds (Staebler et al., submitted manuscript, 2011) that remobilized the surface snow, and thus re-shaped the surface completely, even in the absence of fresh precipitation (Domine et al., submitted manuscript, 2011a).

[51] We distinguish 11 periods, 5 shorter than one day, based on meteorological parameters. The 6 calm periods were of 2 to 12 days duration. The snow surfaces during these calm periods showed a wind crust, on which surface hoar grew and diamond dust deposited steadily (Domine et al., submitted manuscript, 2011b). Figure 11 shows the temporal slopes in

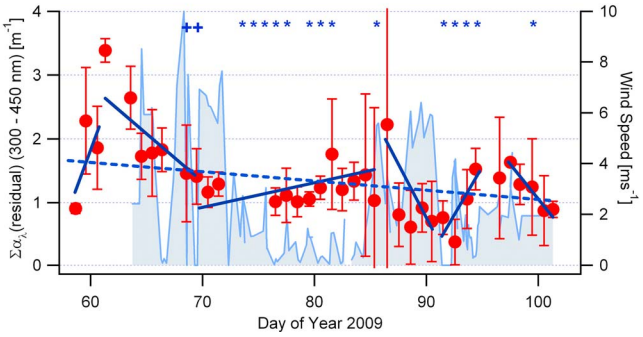

Figure 11. Time series of daily averaged $\Sigma\alpha_\lambda$ (residual) (red circles, with error bars of 1 standard deviation) between 300–450 nm in surface snows (top 5 cm, including surface hoars and diamond dust, where present). Similar time series are also observed at all other wavelength intervals between 220–600nm. The surface layer is mostly influenced by weather; the figure shows the wind speed (blue shaded area, right axis (Staebler et al., submitted manuscript, 2011)) and major snowfalls (blue 'plus' signs at top of figure, while stars denote days where up to 2 mm diamond dust were detected (Domine et al., submitted manuscript, 2011b). Our campaign can be divided into 6 major meteorological periods that show similar winds, temperatures, snowfall, etc. $\Sigma\alpha_\lambda$ (residual) for these periods shows the following slopes: 0.48, −0.18, 0.02, −0.37, 0.33, −0.22 [m^{-1}/day] (slopes shown by solid blue lines, in same order as in figure). In the interest of simplicity, short periods of drastic change are not separately analyzed in this figure. For the entire time period a slope of −0.015 [m^{-1}/day] (rel.std.error 0.00344, p = 0.00003) is statistically significant.

$\Sigma\alpha_\lambda$ (residual) for the 6 major calm periods, which varied from 0.478 to −0.373 m^{-1}/day. Although it seems that slopes are greatest during stronger winds, there is actually no significant relationship with surface wind speed (measured at 60 cm above ground). In conclusion, even though we have evidence for photo-bleaching of chromophores in the snow surface layer, the larger variations in $\Sigma\alpha_\lambda$ (residual) are caused by physical changes to the surface by wind and snow deposition.

3.9. Relationships Between Small Carbonyls, HULIS, and Light Absorption

[52] During our Barrow campaign we also analyzed snow samples for HULIS and small aldehydes [*Barret et al.*, 2011b; Voisin et al., submitted manuscript, 2011], as correlations between these species (and absorption) might help identify the chemical nature of the unknown chromophores. $\Sigma\alpha$ (HULIS) (300–450 nm) in our samples is weakly correlated with glyoxal (slope = 0.95 [$m^{-1}/\mu gL^{-1}$] (standard error = 0.42), p = 0.057), but not with HCHO, CH_3CHO, or methylglyoxal [*Barret et al.*, 2011b; Voisin et al., submitted manuscript, 2011]. Further, *Barret et al.* [2011b] observed increased HCHO at the surface of the snowpack, but there is no clear source for acetaldehyde, glyoxal, or methylglyoxal from the bottom of the snowpack that is in contact with the vegetation.

[53] Both formaldehyde and acetaldehyde are weakly related with $\Sigma\alpha_\lambda$ (residual) between 300–450 nm, with all three parameters being higher in the surface layers. HCHO is significantly correlated with $\Sigma\alpha_\lambda$ (residual) in surface snows (top 1 cm), with a slope of 0.426 [$\mu gL^{-1}/m^{-1}$] (std. error ± 0.16, p = 0.0118); however, samples from the surface hoar layer on top of the wind-crust by themselves show no statistically significant relationship between HCHO and the summed residual absorption coefficient. Glyoxal concentrations, in contrast, were unchanged with depth. Figure 12 suggests a relationship between glyoxal and $\Sigma\alpha_\lambda$ (residual) (300–450 nm) that holds for all sampled layers, with a slope of 0.51 $\mu g\ L^{-1}/m^{-1}$ (std. error ± 0.13, p = 0.00022). Correlations of these organics with H_2O_2 (not shown) do not reveal any significant relationships. HULIS may be a source for small aldehydes, or these organic molecules may share similar sources. Thus a relationship between $\Sigma\alpha_\lambda$ (residual) and aldehydes is expected since the residual chromophores contains on average 50% HULIS. For the few cases that both HULIS and aldehyde data can be compared to our absorption samples, the unknown absorption after subtraction of HULIS fraction $\Sigma\alpha_\lambda$ (unknown) between 300–450 nm shows no statistically significant relationship with either HCHO or glyoxal (auxiliary material Figure S8). However, in the case of HCHO the slope is twice that of HCHO/$\Sigma\alpha_\lambda$ (residual) and *almost* significant. This agrees with increased HCHO at the surface of the snowpack [*Barret et al.*, 2011b], and indicates that HCHO exists or has sources in the snowpack independent of HULIS. Alternatively, the HULIS analysis may not have captured all humic-like material. The lack of a significant correlation with HCHO also confirms that $\Sigma\alpha_\lambda$ (unknown) has a non-terrestrial source, i.e., either maritime (short-range atmospheric), or from longer-range atmospheric transport.

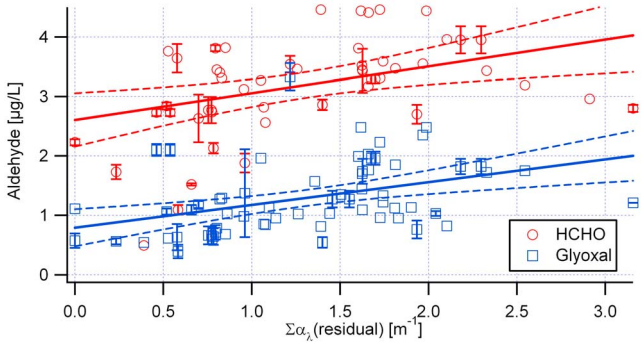

Figure 12. Correlation of the aldehydes HCHO (red circles) and glyoxal (blue squares) with the sum of residual absorptions $\Sigma\alpha_\lambda$ (residual) in the range 300–450 nm. The slopes are 0.426 (std. error ± 0.162, p = 0.0118) HCHO/$\Sigma\alpha_\lambda$ (residual) and 0.513 (std. error ± 0.126, p = 0.00022) glyoxal/$\Sigma\alpha_\lambda$ (residual). Also shown are 95% confidence intervals of the slopes. This figure shows all samples in the top 1 cm layer taken during the entire campaign; however, samples from the very surface layer on top of the wind crust by themselves show no statistically significant slope for HCHO. Further, HCHO data during the 36-h experiment (see section 3.6) are not shown here: they showed no statistically significant relationship with $\Sigma\alpha_\lambda$ (residual) (300–450 nm) and were 50–100% higher than during the rest of the campaign.

3.10. Implications for Snowpack Photochemistry

[54] What do our light absorption results suggest about snowpack photochemistry at Barrow? First, even though nitrate, nitrite, and hydrogen peroxide make only minor contributions to the amount of sunlight absorbed by Barrow snow, their contributions to photochemistry are important: NO_3^- and NO_2^- are important sources of snowpack NO_x, while H_2O_2 and NO_3^- are major sources of OH on snow grains (France et al., submitted manuscript, 2011). Second, our identification of HULIS as a major chromophore in Barrow snow indicates that HULIS-mediated photochemistry is probably important. Because HULIS encompasses a complex and varying suite of molecules in different locations, it is difficult to predict the impact of HULIS photochemistry on Barrow snow grains. However, past work has identified a number of the (photo)chemical pathways involving HULIS in ice and surface waters, including water assisted cooperative sorption of organic compounds onto HULIS, changing their structure [*Taraniuk et al.*, 2009], contribution of atmospheric HULIS to (nighttime) oxidation of organic pollutants in cloud water via the dark (and photo-) Fenton reaction [*Moonshine et al.*, 2008], oxidative photodegradation of HULIS and formation of aryl aldehydes [*Cowen and Al-Abadleh*, 2009], light-induced ozone depletion by HULIS [*D'Anna et al.*, 2009], and its possibly essential role in HONO production from photochemical reactions of NO_3^- in snowpacks [*Beine et al.*, 2008]. Finally, unknown chromophores (i.e., not NO_3^-, NO_2^-, H_2O_2, or HULIS) are responsible for approximately half of sunlight absorption by Barrow snows, implying that there is a significant amount of uncharacterized photochemistry that is occurring in these samples, with possible implications for snowpack cycling of carbon, nitrogen, halogens, and oxidants.

4. Summary

[55] We have identified four main sources for our snowpack chromophores: (1) vegetation and organic debris, which are especially important in the lowest regions of the snowpack, (2) marine inputs that are identified by high Cl^- and SO_4^{2-} content, and which were delivered during strong wind episodes prior to our campaign, (3) atmospheric deposition of diamond dust to the surface, and (4) gas-phase exchange (e.g., of H_2O_2) between the atmosphere and the surface snow layers. The first 2 sources were most active in early winter, before our campaign started; they produced a stratified snowpack with distinct layers.

[56] In contrast to previous work at Summit and Dome C, at Barrow we find that H_2O_2 and NO_3^- make minor contributions to light absorption in snow, while HULIS and unknown chromophores are each responsible for approximately half of absorption. Given that HULIS photochemistry is not well constrained, and we do not know the identities of the unknown chromophores, our light absorption budget suggests that much of the photochemistry in snowpacks is still unknown. We do have evidence, however, that the unknown chromophores at Barrow have a marine source, as we have shown for specific times and snow layers, although we cannot rule out other sources as well. The sources and nature of marine contributions are explored in a companion paper (Beine et al., submitted manuscript, 2011).

[57] **Acknowledgments.** This work is part of the international multidisciplinary OASIS (Ocean-Atmosphere-Sea Ice-Snowpack) program. Funding for this work was gratefully received from NSF ATM-0807702. F.D. also gratefully acknowledges support from the French Polar Institute, IPEV grant 1017-OASIS. We would like to thank Thomas W. Kirchstetter and Odelle Hadley (Lawrence Berkeley National Laboratory) for molar absorptivity values of elemental carbon.

References

Amoroso, A., et al. (2010), Microorganisms in dry polar snow are involved in the exchanges of nitrogen oxides with the atmosphere, *Environ. Sci. Technol.*, *44*, 714–719, doi:10.1021/es9027309.

Anastasio, C., and L. Chu (2009), Photochemistry of nitrous acid (HONO) and nitrous acidium ion (H_2ONO^+) in aqueous solution and ice, *Environ. Sci. Technol.*, *43*(4), 1108–1114, doi:10.1021/es802579a.

Anastasio, C., and T. Robles (2007), Light absorption by soluble chemical species in Arctic and Antarctic snow, *J. Geophys. Res.*, *112*, D24304, doi:10.1029/2007JD008695.

Anastasio, C., E. S. Galbavy, M. A. Hutterli, J. F. Burkhart, and D. Friel (2007), Photoformation of hydroxyl radical on snow grains at Summit, Greenland, *Atmos. Environ.*, *41*, 5110–5121, doi:10.1016/j.atmosenv.2006.12.011.

Barret, M., S. Houdier, and F. Domine (2011a), Thermodynamics of the formaldehyde-water and formaldehyde-ice systems for atmospheric applications, *J. Phys. Chem. A*, *115*(3), 307–317, doi:10.1021/jp108907u.

Barret, M., F. Domine, S. Houdier, J.-C. Gallet, P. Weibring, J. Walega, A. Fried, and D. Richter (2011b), Formaldehyde in the Alaskan Arctic snowpack: Partitioning and physical processes involved in air-snow exchanges, *J. Geophys. Res.*, doi:10.1029/2011JD016038 in press.

Bartels-Rausch, T., M. Brigante, Y. F. Elshorbany, M. Ammann, B. D'Anna, C. George, K. Stemmler, M. Ndour, and J. Kleffmann (2010), Humic acid in ice photo-enhanced conversion of nitrogen dioxide into nitrous acid, *Atmos. Environ.*, *44*(40), 5443–5450, doi:10.1016/j.atmosenv.2009.12.025.

Beine, H., and C. Anastasio (2011), The photolysis of flash-frozen dilute hydrogen peroxide solutions, *J. Geophys. Res.*, *116*, D14302, doi:10.1029/2010JD015531.

Beine, H. J., A. Amoroso, F. Domine, M. King, M. Nardino, A. Ianniello, and J. L. France (2006), Small HONO emissions from snow surfaces at Browning Pass, Antarctica, *Atmos. Chem. Phys.*, *6*, 2569–2580, doi:10.5194/acp-6-2569-2006.

Beine, H., A. J. Colussi, A. Amoroso, G. Esposito, M. Montagnoli, and M. R. Hoffmann (2008), HONO emissions from snow surfaces, *Environ. Res. Lett.*, *3*, 045005, doi:10.1088/1748-9326/3/4/045005.

Bell, R. P. (1966), The reversible hydration of carbonyl compounds, *Adv. Phys. Org. Chem.*, *4*, 1–29, doi:10.1016/S0065-3160(08)60351-2.

Buschmann, H. J., E. Dutkiewicz, and W. Knoche (1982), The reversible hydration of carbonyl compounds in aqueous solution Part II: The Kinetics of the keto/gem-diol transition, *Ber. Bunsenges. Phys. Chem*, *86*(2), 129–134.

Chu, L., and C. Anastasio (2003), Quantum yields of hydroxyl radical and nitrogen dioxide from the photolysis of nitrate on ice, *J. Phys. Chem. A*, *107*, 9594–9602, doi:10.1021/jp0349132.

Chu, L., and C. Anastasio (2005), Formation of hydroxyl radical from the photolysis of frozen hydrogen peroxide, *J. Phys. Chem. A*, *109*, 6264–6271, doi:10.1021/jp051415f.

Chu, L., and C. Anastasio (2007), Temperature and wavelength dependence of nitrite photolysis in frozen and aqueous solutions, *Environ. Sci. Technol.*, *41*(10), 3626–3632, doi:10.1021/es062731q.

Cowen, S., and H. A. Al-Abadleh (2009), DRIFTS studies on the photodegradation of tannic acid as a model for HULIS in atmospheric aerosols, *Phys. Chem. Chem. Phys.*, *11*, 7838–7847, doi:10.1039/b905236d.

D'Anna, B., A. Jammoul, C. George, K. Stemmler, S. Fahrni, M. Ammann, and A. Wisthaler (2009), Light-induced ozone depletion by humic acid films and submicron aerosol particles, *J. Geophys. Res.*, *114*, D12301, doi:10.1029/2008JD011237.

Doherty, S. J., S. G. Warren, T. C. Grenfell, A. D. Clarke, and R. E. Brandt (2010), Light-absorbing impurities in Arctic snow, *Atmos. Chem. Phys.*, *10*, 11,647–11,680, doi:10.5194/acp-10-11647-2010.

Domine, F., and P. B. Shepson (2002), Air-snow interactions and atmospheric chemistry, *Science*, *297*, 1506–1510, doi:10.1126/science.1074610.

Domine, F., R. Sparapani, A. Ianniello, and H. J. Beine (2004), The origin of sea salt in snow on Arctic sea ice and in coastal regions, *Atmos. Chem. Phys.*, *4*, 2259–2271, doi:10.5194/acp-4-2259-2004.

Domine, F., M. Albert, T. Huthwelker, H.-W. Jacobi, A. A. Kokhanovsky, M. Lehning, G. Picard, and W. R. Simpson (2008), Snow physics as

relevant to snow photochemistry, *Atmos. Chem. Phys.*, *8*, 171–208, doi:10.5194/acp-8-171-2008.

France, J. L., M. D. King, J. Lee-Taylor, H. J. Beine, A. Ianniello, and F. Domine (2011), Estimations of in-snow NO_x and OH photochemical production and photolysis rates: A field and radiative-transfer study of the optical properties of Svalbard (Ny-Ålesund) snowpacks, *J. Geophys. Res.*, doi:10.1029/2011JF002019 in press.

Galbavy, E. S., C. Anastasio, B. L. Lefer, and S. R. Hall (2007a), Light penetration in the snowpack at Summit, Greenland: Part 1: Nitrite and hydrogen peroxide photolysis, *Atmos. Environ.*, *41*, 5077–5090, doi:10.1016/j.atmosenv.2006.04.072.

Galbavy, E. S., C. Anastasio, B. L. Lefer, and S. R. Hall (2007b), Light penetration in the snowpack at Summit, Greenland: Part 2. Nitrate photolysis, *Atmos. Environ.*, *41*(24), 5091–5100, doi:10.1016/j.atmosenv.2006.01.066.

George, C., R. S. Strekowski, J. Kleffmann, K. Stemmler, and M. Ammann (2005), Photoenhanced uptake of gaseous NO_2 on solid organic compounds: A photochemical source of HONO?, *Faraday Discuss.*, *130*, 195–210, doi:10.1039/B417888M.

Graber, E. R., Y. Rudich (2006), Atmospheric HULIS: How humic-like are they? A comprehensive and critical review, *Atmos. Chem. Phys.*, *6*, 729–753, doi:10.5194/acp-6-729-2006.

Grannas, A. M., P. B. Shepson, and T. R. Filley (2004), Photochemistry and nature of organic matter in Arctic and Antarctic snow, *Global Biogeochem. Cycles*, *18*(1), GB1006, doi:10.1029/2003GB002133.

Grannas, A. M., W. C. Hockaday, P. G. Hatcher, L. G. Thompson, E. Mosley-Thompson (2006), New revelations on the nature of organic matter in ice cores, *J. Geophys. Res.*, *111*, D04304, doi:10.1029/2005JD006251.

Grannas, A. M., et al. (2007), An overview of snow photochemistry: Evidence, mechanisms and Impacts, *Atmos. Chem. Phys.*, *7*, 4329–4373, doi:10.5194/acp-7-4329-2007.

Grenfell, T. C., and S. G. Warren (2009), Expeditions to the Russian Arctic to survey black Carbon in snow, *Eos Trans. AGU*, *90*(43), 386, doi:10.1029/2009EO430002.

Hagler, G. S. W., M. H. Bergin, E. A. Smith, J. E. Dibb, C. Anderson, and E. J. Steig (2007), Particulate and water-soluble carbon measured in recent snow at Summit, Greenland, *Geophys. Res. Lett.*, *34*, L16505, doi:10.1029/2007GL030110.

Henaff, P. L. (1968), Methodes d'etude et proprietes des hydrates, hemiacetals des aldéhydes et des cetones, *Bull. Soc. Chim. France*, *11*, 4687–4698.

Houdier, S., S. Perrier, F. Domine, A. Cabanes, L. Legagneux, A. M. Grannas, C. Guimbaud, P. B. Shepson, H. Boudries, and J. W. Bottenheim (2002), Acetaldehyde and acetone in the Arctic snowpack during the ALERT2000 campaign. Snowpack composition, incorporation processes and atmospheric impact, *Atmos. Environ.*, *36*(15–16), 2609–2618, doi:10.1016/S1352-2310(02)00109-7.

Hutterli, M. A., J. R. McConnell, R. W. Stewart, H.-W. Jacobi, and R. C. Bales (2001), Impact of temperature-driven cycling of hydrogen peroxide (H_2O_2) between air and snow on the planetary boundary layer, *J. Geophys. Res.*, *106*(D14), 15,395–15,404, doi:10.1029/2001JD900102.

Jacobi, H.-W., M. Frey, M. A. Hutterli, R. C. Bales, O. Schrems, N. J. Cullen, K. Steffen, and C. Koehler (2002), Measurements of hydrogen peroxide and formaldehyde exchange between the atmosphere and surface snow at Summit, Greenland, *Atmos. Environ.*, *36*, 2619–2628, doi:10.1016/S1352-2310(02)00106-1.

King, M. D., J. L. France, F. N. Fisher, and H. J. Beine (2005), Measurement and modelling of UV radiation penetration and photolysis rates of nitrate and hydrogen peroxide in Antarctic sea ice: An estimate of the production rate of hydroxyl radicals in first-year sea ice, *J. Photochem. Photobiol. A: Chem*, *176*, 39–49, doi:10.1016/j.jphotochem.2005.08.032.

Kok, G. L., S. E. McLaren, and T. A. Staffelbach (1995), HPLC determination of atmospheric organic hydroperoxides, *J. Atmos. Oceanic Technol.*, *12*(2), 282–289, doi:10.1175/1520-0426(1995)012<0282:HDOAOH>2.0.CO;2.

Kurz, J. L. (1967), Hydration of acetaldehyde. I. Equilibrium thermodynamic parameters, *J. Am. Chem. Soc.*, *89*(14), 3524–3528, doi:10.1021/ja00990a032.

Lee-Taylor, J., and S. Madronich (2002), Calculation of actinic fluxes with a coupled atmosphere-snow radiative transfer model, *J. Geophys. Res.*, *107*(D24), 4796, doi:10.1029/2002JD002084.

Li, S. M. (1993), Particulate and snow nitrite in the spring Arctic troposphere, *Atmos. Environ.*, *27*(17–18), 2959–2967.

Liu, Y., I. El Haddad, M. Scarfogliero, L. Nieto-Gligorovski, B. Temime-Roussel, E. Quivet, N. Marchand, B. Picquet-Varrault, and A. Monod (2009), In-cloud processes of methacrolein under simulated conditions - Part 1: Aqueous phase photooxidation, *Atmos. Chem. Phys.*, *9*(14), 5093–5105, doi:10.5194/acp-9-5093-2009.

Malik, M., and J. A. Joens (2000), Temperature dependent near-UV molar absorptivities of glyoxal and gluteraldehyde in aqueous solution, *Spectroch. Acta A Mol. Biomol. Spectrosc.*, *56*(14), 2653–2658.

Matykiewiczová, N., R. Kurková, J. Klánová, and P. Klán (2007), Photochemically induced nitration and hydroxylation of organic aromatic compounds in the presence of nitrate or nitrite in ice, *J. Photochem. Photobiol. Chem.*, *187*, 24–32, doi:10.1016/j.jphotochem.2006.09.008.

Montoya, M. R., and J. M. R. Mellado (1994), Use of convolutive potential sweep voltammetry in the calculation of hydration equilibrium constants of α-dicarbonyl compounds, *J. Electroanal. Chem.*, *370*(1–2), 183–187, doi:10.1016/0022-0728(93)03203-2.

Moonshine, M., Y. Rudich, S. Katsman, and E. R. Graber (2008), Atmospheric HULIS enhance pollutant degradation by promoting the dark Fenton reaction, *Geophys. Res. Lett.*, *35*, L20807, doi:10.1029/2008GL035285.

Nemet, I., D. Vikić-Topić, and L. Varga-Defterdarović (2004), Spectroscopic studies of methylglyoxal in water and dimethylsulfoxide, *Bioorg. Chem.*, *32*, 560–570, doi:10.1016/j.bioorg.2004.05.008.

Perrier, S., S. Houdier, F. Domine, A. Cabanes, L. Legagneux, A. L. Sumner, and P. B. Shepson (2002), Formaldehyde in Arctic snow: Incorporation into ice particles and evolution in the snowpack, *Atmos. Environ.*, *36*(15–16), 2695–2705, doi:10.1016/S1352-2310(02)00110-3.

Sander, S. P., et al. (2006), Chemical kinetics and photochemical data for use in atmospheric studies, evaluation number 15, *JPL Publ.*, *06–2*, 523 .

Sham, Y. Y., and J. A. Joens (1995), Temperature-dependent near UV molar absorptivities of several small aldehydes in aqueous-solution, *Spectrochim, Acta A Mol. Biomol. Spectrosc.*, *51*(2), 247–251.

Simpson, W. R., M. D. King, H. Beine, and R. E. Honrath (2002), Atmospheric photolysis rates during the Polar Sunrise Experiment ALERT200 field campaign, *Atmos. Environ.*, *36*, 2471–2480, doi:10.1016/S1352-2310(02)00123-1.

SPSS, Inc. (1999), SYSTAT 9.0 [software], Chicago, Ill.

Taraniuk, I., Y. Rudich, and E. R. Graber (2009), Hydration-influenced sorption of organic compounds by model and atmospheric humic-like substances (HULIS), *Environ. Sci. Technol.*, *43*(6), 1811–1817, doi:10.1021/es802188n.

Thomas, J. L., J. Stutz, B. Lefer, L. G. Huey, K. Toyota, J. E. Dibb, and R. von Glasow (2010), Modeling chemistry in and above snow at Summit, Greenland–Part 1: Model description and results, *Atmos. Chem. Phys. Discuss.*, *10*, 30,927–30,970, doi:10.5194/acpd-10-30927-2010.

Warren, S. G. (1982), Optical properties of snow, *Rev. Geophys.*, *20*, 67–89, doi:10.1029/RG020i001p00067.

Wasa, T., and S. Musha (1970), Polarographic behaviour of glyoxal and its related compounds, *Bull. Osaka Prefect. Univ., Ser. A*, *19*, 169–180.

C. Anastasio, H. Beine, and K. Patten, Department of Land, Air, and Water Resources, University of California at Davis, One Shields Ave., Davis, CA 95616, USA. (hbeine@ucdavis.edu)

M. Barret, S. Houdier, and D. Voisin, Laboratoire de Glaciologie et Géophysique de l'Environnement, CNRS-INSU, BP 96, F-38402 Saint-Martin d'Hères CEDEX, France.

F. Domine, CNRS UMI 3376 Takuvik, Université Laval, Pavillon Alexandre Vachon, Québec, QC G1V 0A6, Canada.

G. Esposito, CNR – IIA, Via Salaria Km 29,300, Monterotondo, I-00015 Rome, Italy.

S. Hall, Atmosphere and Chemistry Division, NCAR, 3090 Center Green Dr., Boulder, CO 80301, USA.

E. Wilkening, Wilson K8 School, 2330 W Glover Rd., Tucson, AZ 85742, USA.